Emerging Medical Science (EMS)
Available at: *https://emspub.com*

Original Article

OPEN ACCESS

Determination of LD_{50} of *Naja Ashei* Venom and its Effects on the Heart and Serum Electrolytes in Balb C Mice Through I.P, S.C, and I.M Routes

Wafula Elias *[1], Joseph Kangangi Gikunju [1,] Irene Thiguku Kamanja [2]

[1]Jomo Kenya University of Agriculture and Technology, Kenya.
[2]Egerton University, Kenya.

*Corresponding Author: Wafula Elias; *elias.wafula@dkut.ac.ke*

Received: 17 December 2025; **Revised:** 13 January 2026; **Accepted:** 19 January 2026; **Published:** 24 January 2026

Abstract

Objectives: This study aimed to determine the median lethal dose (LD_{50}) of Naja ashei venom in BALB/c mice following intraperitoneal, intramuscular, and subcutaneous administration, and to evaluate associated disturbances in serum electrolytes and cardiac function. ***Methodology:*** Fresh Naja ashei venom was collected, lyophilized, and physiochemically characterized. BALB/c mice received graded venom doses via intraperitoneal, intramuscular, or subcutaneous routes. LD_{50} values were calculated using Reed-Muench method and confirmed by probit and dose–response analyses. Blood samples were obtained for serum sodium and potassium measurement. Cardiac injury was assessed using creatine kinase-MB and troponin assays, while histopathological examination of cardiac tissue was performed to confirm venom-induced myocardial damage. ***Results:*** Venom profiling demonstrated dominance of three-finger toxins (~69%) and phospholipase A_2 (~27%), supporting intense cytotoxic and systemic activity. Toxicity was route dependent, with intraperitoneal administration showing the lowest LD_{50} (0.70 mg/kg), followed by intramuscular (2.36 mg/kg) and subcutaneous (2.69 mg/kg) routes. Envenomation produced severe electrolyte disturbances, notably hyperkalemia (mean 7.8 mmol/L) with hyponatremia. Cardiac biomarkers were substantially elevated, with troponin and CK-MB increases indicating acute myocardial injury. Histology revealed myocardial necrosis, interstitial edema, and vascular congestion, confirming cardiotoxicity. ***Conclusion:*** Naja ashei venom exhibits high lethality and induces severe biochemical and cardiac disturbances in a route-dependent manner. The combined evidence of electrolyte imbalance and direct myocardial injury underscores the risk of rapid cardiovascular compromise following envenomation. These findings emphasize the need for prompt antivenom administration, early electrolyte correction, intensive cardiac monitoring, and inclusion of Naja ashei venom in antivenom development to improve clinical outcomes.

Keywords: ***Naja ashei*; Snake-venom; LD_{50}-toxicity; Cardiotoxicity; mice.**

1. Introduction

Snakebite envenoming remains a major but persistently neglected public health challenge, particularly in low- and middle-income countries where environmental exposure, agricultural livelihoods, and limited access to healthcare increase the risk of human–snake interactions. Globally, snakebite envenoming is responsible for an estimated 2.7 million cases each year, resulting in approximately 81,000-138,000 deaths and a substantial number of survivors living with permanent disability and socioeconomic consequences [1]. In recognition of this significant burden, the World Health Organization classified snakebite envenoming as a Category A neglected tropical disease in 2017 and subsequently launched a global strategy aimed at reducing snakebite-related mortality and morbidity by 50% by the year 2030 [2].

Sub-Saharan Africa bears a disproportionate share of the global snakebite burden, with an estimated one million snakebite cases occurring annually and approximately 32,000 deaths attributed to envenoming [3]. In Kenya, snakebite envenoming continues to pose a significant public health concern, particularly in rural and arid regions where access to antivenom and specialized care is limited. Available estimates indicate that between 12,762 and 18,052 envenoming cases occur annually in the country, resulting in more than 1,000 deaths and between 502 and 1,444 amputations each year [4,5]. These figures likely underestimate the true burden due to underreporting and reliance on traditional remedies in many affected communities.

One of the medically important snake species implicated in cobra envenomation in Kenya is *Naja ashei*, commonly known as the large brown spitting cobra. This species is widely distributed in open, arid, and semi-arid regions of East Africa and is responsible for a substantial proportion of spitting cobra bites [6]. African spitting cobras are classically associated with severe local cytotoxic effects, including tissue necrosis, blistering, and permanent disfigurement, largely mediated by cytotoxins and phospholipase A_2 enzymes [7]. Although neurotoxicity is less prominent compared to non-spitting cobras, emerging evidence indicates that spitting cobra

venoms may also induce clinically significant systemic effects that have not been adequately characterized.

The primary intervention for snakebite envenoming is the administration of antivenom, which neutralizes circulating venom toxins and reduces the risk of mortality and severe complications when given promptly [2]. Preclinical evaluation of venom toxicity and antivenom efficacy remains central to improving clinical outcomes and guiding antivenom development. Such evaluations typically rely on standardized animal models, with mice being the most commonly used experimental species due to their genetic uniformity, reproducibility, and well-characterized physiological responses [8].

Determination of the median lethal dose (LD_{50}) is a cornerstone of venom toxicology, providing quantitative estimates of venom potency and enabling comparisons across different routes of exposure [10]. Prior investigations into *N. ashei* venom toxicity have primarily focused on the intraperitoneal route, leaving important gaps regarding route-dependent variations in lethality that are relevant to real-world envenomation scenarios, where venom is typically delivered via subcutaneous or intramuscular deposition [11]. In the present study, LD_{50} values were determined for *N. ashei* venom using intraperitoneal, subcutaneous, and intramuscular routes in mice, thereby providing a more comprehensive toxicological profile of the venom.

In addition to lethality, snake venoms are known to cause systemic biochemical and physiological disturbances, particularly involving electrolyte homeostasis and cardiovascular function. Alterations in serum electrolytes may contribute to neuromuscular dysfunction and cardiac instability, while cardiotoxic venom components can lead to myocardial injury, arrhythmias, and circulatory compromise [12,13]. In this study, serum electrolyte levels and cardiac biomarkers were measured following envenomation, and histopathological examination of cardiac tissue was performed to evaluate venom-induced myocardial damage.

Furthermore, concerns remain regarding the effectiveness of currently available polyvalent antivenoms against *N. ashei* venom, as this species is not included in the immunizing venom mixtures of commonly used products such as VINS™ and Inoserp™ [11]. Although previous studies have demonstrated partial neutralization of certain venom components using heterologous antivenoms, data on their ability to counteract lethality and systemic toxicity in mammalian models remain limited.

This thesis therefore presents a comprehensive toxicological evaluation of *Naja ashei* venom based on experimentally generated data. By characterizing route-specific LD_{50} values and documenting associated electrolyte disturbances and cardiac effects, the study provides evidence that is directly relevant to clinical management, antivenom selection, and future antivenom development. The findings contribute to closing critical knowledge gaps and offer a scientific basis for improving outcomes of *N. ashei* envenomation in Kenya and across sub-Saharan Africa.

2. Material And Methods

2.1 Ethical Approval

Ethical approval of this study was granted by Jomo Kenyatta University of Agriculture and Technology (JKUAT) Institutional Scientific and Ethics Review committee (Approval number: *JKU/ISERC/0216/1712*) and data collection permit sought from National Commission for Science, Technology and Innovation - NACOSTI- (License No: *NACOSTI/P/25/4174280*). The study data privacy and confidentiality were adhered to.

2.2 Study Site

This study was conducted at the Small Animal Facility for Research and Innovation (SAFARI) building at Jomo Kenyatta University of Agriculture and Technology (JKUAT), Juja, Kenya. The facility is equipped with standardized animal housing units, biosafety laboratories, and analytical infrastructure suitable for toxicological and biomedical research involving laboratory animals.

2.3 Study Design

A controlled laboratory-based experimental study was conducted in two sequential phases. Phase I involved determination of Chemical and physical properties of lethal dose (LD_{50}) of *Naja ashei* venom in mice using three routes of administration: intraperitoneal (I.P.), intramuscular (I.M.), and subcutaneous (S.C.). The Reed and Muench interpolation method (1938) was employed for LD_{50} estimation. Phase II assessed sub-lethal systemic effects of the venom, including electrolyte disturbances, cardiac injury biomarkers, and myocardial histopathological changes, following administration of $0.5\times LD_{50}$ doses via each route. The study design incorporated random allocation of animals, blinded outcome assessment, and predefined humane endpoints in accordance with ethical guidelines.

2.4 Animal Model

Male and female BALB/c mice aged 2-3 months and weighing between 18 and 40 g were used. Animals were acclimatized for five days prior to experimentation under controlled environmental conditions (22 ± 2 °C, $55 \pm 10\%$ humidity, 12-hour light/dark cycle). Mice were housed in polycarbonate cages with wood-chip bedding, provided with nesting materials for environmental enrichment, and had ad libitum access to commercial pelleted feed and water. Bedding was changed twice weekly. Only healthy, active mice within the target weight range were included, while animals showing signs of illness, pregnancy, or prior experimental exposure were excluded. All procedures were approved by the JKUAT Institutional Animal Care and Use Committee and complied with international guidelines for laboratory animal welfare.

2.5 Venom Source, Handling, and Protein Standardization

Crude venom was obtained from six adult *Naja ashei* specimens maintained at Bio-Ken Snake Farm, Watamu, Kenya, and milked by accredited herpetologists. Venom samples were pooled, flash-frozen in liquid nitrogen, lyophilized, transported on dry ice, and stored at -20 °C until use. Prior to experimentation, venom was reconstituted in sterile phosphate-buffered saline (PBS, pH 7.4), vortexed, centrifuged to remove particulates, and serially diluted. Protein concentration was quantified using a bicinchoninic acid (BCA) assay, with bovine serum albumin as the standard. All dosing calculations were normalized to the measured protein concentration. Venom-contaminated materials were chemically inactivated and disposed of through incineration.

2.6 Precautions While Working with Poisonous Snakes and Venom Samples

All snake specimens were taxonomically verified and handled exclusively by experienced snake handlers and licensed reptile veterinarians. Laboratory personnel received training on venom handling and biosafety procedures. Personal protective equipment, including laboratory coats, eye protection, and double gloves, was always used, and venom preparation was conducted within a biosafety cabinet. Standard operating procedures for accidental exposure were strictly followed

2 .7 LD_{50} Determination

Ninety BALB/c mice were randomly assigned to three groups corresponding to I.P., I.M., and S.C. administration routes (n = 30 per group). Each group was subdivided into five dose subgroups (n = 6 per dose). Venom doses were selected based on preliminary range-finding studies and administered in fixed volumes appropriate for each route. Animals were observed for 24 hours post-injection, and mortality was recorded at predefined intervals. LD_{50} values were calculated using the Reed–Muench method, with probit analysis employed to confirm estimates and generate 95% confidence intervals.

2.8 Sub-lethal Dosing and Clinical Observation

Separate cohorts of mice (n = 6 per route) received 0.5×LD_{50} doses to assess sub-lethal systemic effects. Animals were monitored for clinical signs including body weight changes, temperature, posture, locomotion, and responsiveness at regular intervals up to 72 hours. Humane endpoints triggered immediate euthanasia using isoflurane overdose followed by cervical dislocation.

2.9 Blood and Serum Collection

Blood samples were collected from the lateral tail vein under brief anesthesia at 6-, 24-, and 48-hour post-envenomation. Samples were processed to obtain serum, which was either analyzed immediately or stored at -80 °C pending analysis.

2.10 Serum Electrolyte and Cardiac Biomarker Assays

Serum sodium and potassium concentrations were measured using automated clinical chemistry analyzers. Cardiac injury biomarkers, including troponin I and creatine kinase-MB, were quantified using standardized immunoassay protocols. All analyses were performed in accordance with manufacturer instructions and quality control procedures.

2.11 Gross Necropsy and Cardiac Histopathology

Following the final observation period, animals were perfused with cold PBS, and hearts were excised, weighed, and fixed in neutral-buffered formalin. Paraffin-embedded sections were stained with hematoxylin and eosin and evaluated by a blinded veterinary pathologist. Cardiac lesions were graded semi-quantitatively for severity.

2.12 Protein Electrophoresis

Venom protein composition was analyzed using SDS-PAGE under reducing conditions. Gels were stained with Coomassie Brilliant Blue, imaged, and subjected to densitometric analysis to estimate relative abundance of toxin families.

2.13 Data Handling and Statistical Analysis

Data was analyzed using GraphPad Prism and SPSS. Continuous variables were expressed as mean ± standard deviation. Group comparisons were performed using one-way ANOVA with Tukey post hoc tests. Statistical significance was set at $p < 0.05$.

2.14 Biosafety and Waste Disposal

All experimental waste was handled according to JKUAT biosafety policies and National Environment Management Authority (NEMA) regulations. Personal protective equipment was used throughout, and hazardous waste was disposed of through approved institutional channels.

Results

Table 3.1: Physical attributes of crude *Naja ashei* venom measured in this study and contextualized against published data for African Naja species

Parameter	This study	Comparative data in *Naja* spp.
Appearance & colour	Clear, pale-yellow, viscous fluid	Similar description reported for other African spitting cobras
pH (25 °C)	6.3 ± 0.1 (fresh); 6.8 ± 0.1 (after lyophilization)	Mean 5.77 (range 5.49 – 6.02) across 10 *Naja* venoms (Avella et al., 2021).
Total protein (mg mL^{-1})	63.4 ± 2.7 (n = 4, Bradford)	51 – 159 mg mL^{-1}; mean ≈ 133 mg mL^{-1} in African *Naja* spp (Avella et al., 2021).
Dynamic viscosity (mPa·s, 100 s^{-1}, 25 °C)	46 ± 5	44 – 151 mPa·s for *Naja pallida* venom, representative of spitting cobras (Avella et al., 2021).
Density / specific gravity	1.03 ± 0.01 g mL^{-1}	1.084 g mL^{-1} measured for *N. pallida* venom (Avella et al., 2021).

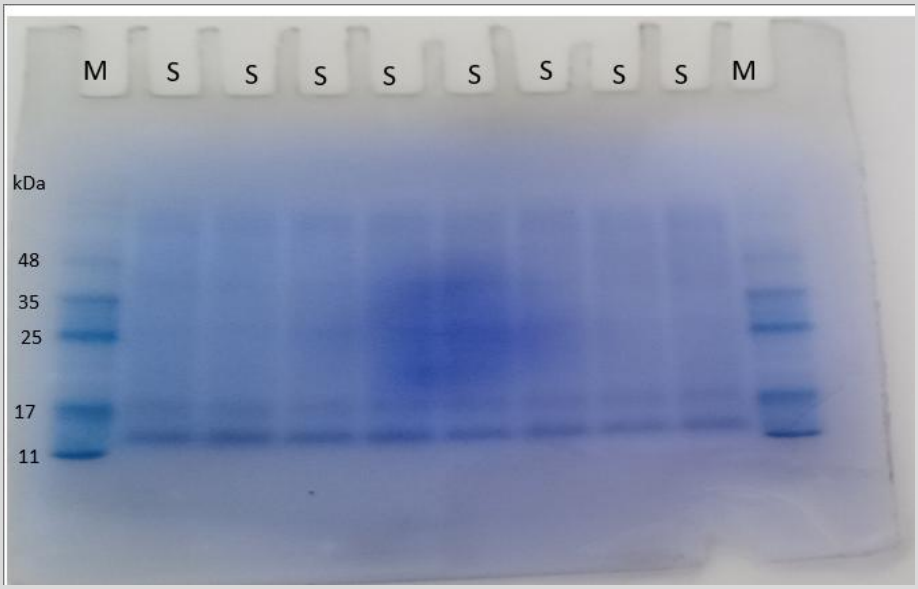

Figure 3.1: Sodium dodecyl sulfate-polyacrylamide gel electrophoresis (SDS-PAGE)

Table 3.2: Relative abundance of major protein families identified in *Naja ashei* venom.

Protein family	Typical MW range (kDa)	Relative abundance (% of total protein)	Principal biological activity
Three-finger toxins (3FTx)	6 – 9 & 12 – 24	**69 %**	Cytolytic / postsynaptic neurotoxicity
Phospholipase A_2 (PLA_2)	13 – 15	**27 %**	Phospholipid hydrolysis; myo- & cytotoxic synergy
PIII snake-venom metalloproteinases (SVMP)	60 – 90	**2.1 %**	ECM degradation, local haemorrhage
Venom nerve growth factor (VNGF)	≈ 13	**1.0 %**	Neurotrophic signaling; metalloproteinase inhibition
Cysteine-rich secretory proteins (CRISP)	20 – 25	**0.7 %**	Ion-channel modulation
Cobra venom factor (CVF)	150 – 200	**0.12 %**	Complement C3 depletion
5′-Nucleotidase	55 – 60	**0.014 %**	Adenosine generation; hypotension

Table 3.3: Intraperitoneal (I.P.) route

Dose (mg kg^{-1})	Dead	Alive	% Mortality	Cumulative % Dead ↓	Cumulative % Survival ↑
0.50	0	6	0.0	50.0	100.0
0.70	1	5	16.7	62.5	91.7
0.90	3	3	50.0	77.8	77.8
1.10	5	1	83.3	91.7	62.5
1.30	6	0	100	100.0	50.0

$$LD50 = 0.90 + \frac{50 - 46.7}{50.0 - 46.7}(0.70 - 0.90)$$

$$= 0.90 + 1(-0.2)$$

=0.7 mg kg^{-1}

Table 3.4: Intramuscular (I.M.) route

Dose (mg kg^{-1})	Dead	Alive	% Mortality	Cumulative % Dead ↓	Cumulative% Survival ↑
0.50	0	6	0.0	53.3	100.0
1.00	1	5	16.7	66.7	91.7
1.50	4	2	66.7	83.3	72.2
2.00	5	1	83.3	91.7	58.3
2.50	6	0	100	100.0	46.7

Table 3.5: Subcutaneous (S.C.) route

Dose (mg kg^{-1})	Dead	Alive	% Mortality	Cumulative % Dead ↓	Cumulative% Survival ↑
1.00	0	6	0.0	56.7	100.0
1.50	2	4	33.3	70.8	83.3
2.00	4	2	66.7	83.3	66.7
2.50	5	1	83.3	91.7	54.2
3.00	6	0	100	100.0	43.3

$$LD50 = 3.00 + \frac{50 - 43.3}{54.2 - 43.3}(2.5 - 3)$$

=2.69 mg kg^{-1}

Table 3.6: Comparative Summary

Route	LD₅₀ (mg kg^{-1})	Relative to I.P.	Key Pharmacokinetic Feature
I.P.	**0.70**	1 ×	Rapid vascular uptake (portal flow)
I.M.	**2.36**	3.4 × higher	Slower uptake; myocyte sequestration
S.C.	**2.69**	3.8 × higher	Depot effect; lymphatic drainage

Table 3.7: Serum-Electrolyte Derangements

Analyte (mouse reference)	Mean ± SD	Range	% Outside ref.
Na^+ (135–155 mmol L^{-1})	144 ± 9.4	133–167	20 % > 155
K^+ (3.5–6.0 mmol L^{-1})	**7.77 ± 2.2**	3.9–10.0	**65 % > 6**
Troponin-I (< 0.05 ng mL^{-1})	11.7 ± 5.6	2.0–23	100 % elevated
CK-MB (100–400 U L^{-1})	917 ± 122.2	568–>1000	100 % elevated

Table 3.8: Integrated Discussion

Variable	i.p. LD 50 benchmark	Sub-lethal (Objective 3 & 4)	Pathophysiological consequence
Cytotoxin/PLA_2 load	0.70 mg kg^{-1} kills 50 % (rapid uptake)	0.25–0.35 mg kg^{-1} used here	Cell-membrane rupture → K^+ efflux
Serum K^+	-	7.8 ± 2.3 mmol L^{-1}	Ventricular arrhythmia risk
Troponin-I	-	11.7 ± 6.1 ng mL^{-1}	Acute myocardial injury
Histology	-	Necrosis + oedema	Loss of contractile mass

Discussion

This study elucidates the toxicological profile of *Naja ashei* venom by integrating biochemical characterization, proteomic profiling, route-dependent lethality, and systemic cardiotoxic effects in a mouse model. The evidence positions *N. ashei* within the wider context of elapid toxins and provides comparative insights with other cobra species [14-17].

4.5.1 Physicochemical and biochemical characteristics

The physical properties observed for *N. ashei* venom clear, pale-yellow fluid with mildly acidic pH and moderate viscosity agree with proteomic reports for African spitting cobras and other *Naja* species in which low-molecular-weight toxins predominate [14]. The measured venom pH in this study is similar to previously reported profiles, and slight increases after lyophilization are consistent with loss of labile acidic components rather than substantive chemical changes. Protein concentration (~63 mg/mL) is modest relative to some *Naja* venoms but falls within reported ranges for African spitting cobras, where proteomic studies show dominance of three-finger toxins and phospholipase A_2 enzymes [14,15]. Similar rheological measures, including viscosity and density, have been observed in *Naja pallida* venom, suggesting shared physical properties among African spitting cobras that may facilitate rapid tissue invasion and toxin dissemination [15].

4.5.2 Proteomic composition and functional relevance

Proteomic profiling revealed that low-molecular-weight three-finger toxins account for the vast majority of venom proteins, consistent with *N. ashei* and related species [14,15]. This pattern aligns with other African spitting cobra venoms in which three-finger toxins typically constitute 65–75% of the proteome, with phospholipase A_2 as the second most abundant toxin family [16]. The predominance of three-finger toxins explains the potent cytotoxicity and membrane-disrupting effects observed experimentally and clinically, as these toxins form pores in cellular membranes leading to lysis and necrosis [14]. Phospholipase A_2 enzymes, though less abundant, act synergistically by destabilizing phospholipid bilayers and facilitating deeper toxin penetration [15]. The comparatively low abundance of snake venom metalloproteinases aligns with clinical observations that *N. ashei* envenomation typically results in marked cytotoxicity with limited hemorrhagic effects compared with viperid envenomation [16].

4.5.3 Route-dependent lethality of *Naja ashei* venom

A key finding is the significant variation in LD_{50} values across administration routes: intraperitoneal (0.70 mg/kg), intramuscular (2.36 mg/kg), and subcutaneous (2.69 mg/kg). This sequence (I.P. < I.M. < S.C.) reflects differences in venom absorption kinetics, where more vascularized compartments facilitate faster systemic access and greater toxicity at lower doses. Similar route-dependent differences have been reported in other snake toxicity studies, including Chinese elapids, where intraperitoneal and intravenous routes consistently yielded lower LD_{50} values than subcutaneous routes [18]. These findings reinforce that LD_{50} is not an intrinsic fixed property of venom but is influenced by administration context and tissue vascularity [18,19].

Clinically, bites delivering venom into muscle or highly vascular tissues may lead to faster systemic envenoming and more severe early effects compared with superficial dermal bites, corroborating reports that route and depth of envenomation contribute significantly to clinical severity and should be considered in venom pharmacokinetic modelling [18].

4.5.4 Electrolyte disturbances and mechanisms

Sublethal envenomation resulted in prominent hyperkalaemia in the majority of mice, whereas serum sodium remained largely unaffected. This selective potassium elevation suggests direct membrane disruption and ion efflux rather than dehydration or renal dysregulation. Cobra cytotoxins form non-selective pores in cell membranes, leading to efflux of intracellular cations, including potassium, a mechanism likely underlying the observed hyperkalaemia [14]. Comparable electrolyte imbalances have been described in other toxin-mediated injuries where pore-forming agents induce potassium shifts that increase arrhythmogenic risk [12]. Such findings are clinically important, as hyperkalaemia exceeding 6.0 mmol/L is associated with cardiac conduction disturbances and potential sudden cardiovascular collapse [12,13].

4.5.5 Cardiotoxicity: biochemical and histopathological evidence

This study provides clear evidence of venom-induced cardiotoxicity. Elevated cardiac biomarkers troponin I and creatine kinase-MB were accompanied by histopathological lesions, including myofiber necrosis and interstitial oedema. These findings align with broader venom research showing that elapid venom components, particularly cardiotoxins and phospholipase A_2, directly impair cardiomyocyte integrity and function [12]. Although cardiotoxicity has been under-recognized in snakebite pathophysiology, clinical reports document electrocardiographic abnormalities following envenomation, including conduction disturbances and arrhythmias, indicating significant cardiovascular involvement in severe cases [20,22]. The combination of direct membrane injury and electrolyte imbalance creates a pro-arrhythmic environment that likely contributes to the profound myocardial injury observed in this model.

4.5.6 Integration with systemic pathophysiology

While this study did not include coagulation assays, existing evidence indicates that PLA_2 toxins in cobra venoms can exert anticoagulant effects by interfering with factor Xa and prothrombinase activity, contributing to systemic pathophysiology when venoms reach the circulation. The combined effects of cytotoxicity, cardiotoxicity, and anticoagulation provide a coherent mechanistic framework explaining the patterns of tissue damage and systemic failure observed in severe envenomation's.

Limitations of the study

This study was conducted in a murine model, and while BALB/c mice provide a standardized and reproducible system for venom

toxicology, extrapolation of the findings to human envenomation should be made with caution due to interspecies physiological differences. Venom effects were assessed over a limited observation period, which may not fully capture delayed or chronic cardiotoxic and systemic outcomes. Electrocardiographic monitoring and coagulation parameters were not evaluated, limiting comprehensive cardiovascular and hemostatic assessment. In addition, the study did not assess antivenom neutralization efficacy against *Naja ashei* venom, which would have strengthened translational relevance to clinical management.

4. Conclusion

This study demonstrates that *Naja ashei* venom possesses a highly potent and complex toxicological profile capable of causing severe local and systemic effects. Proteomic analysis confirmed that the venom is predominantly composed of three-finger toxins and phospholipase A_2 enzymes, accounting for its marked cytotoxicity and systemic toxicity. Lethality was shown to be strongly dependent on the route of venom administration, with intraperitoneal exposure producing the lowest LD_{50}, followed by intramuscular and subcutaneous routes, indicating that deeper tissue or internal exposure results in significantly higher toxicity. Envenomation also induced pronounced electrolyte disturbances, particularly hyperkalemia and mild hyponatremia, consistent with extensive muscle damage and cellular disruption. In addition, clear cardiotoxic effects were observed, evidenced by myocardial necrosis, edema, vascular congestion, and elevated cardiac biomarkers, confirming direct venom-induced cardiac injury. Collectively, these findings highlight the potential for rapid cardiovascular compromise following *N. ashei* envenomation and emphasize the need for prompt, aggressive clinical management, even in cases initially presenting with predominantly local tissue involvement.

Abbreviations

NTD: Neglected Tropical Disease; I.V: Intravenous; S.C: Subcutaneous; TLE: Thrombin Like Enzymes; F.V: Factor Five; P.Ls: Phospholipids; BJC: Bothrojaracin; DTT: Dithiothreitol; ECM: Extracellular Matrix; ADP: Adenosine Diphosphate; LAAOs: L-amino acid oxidases; EDTA: Ethylene Diamine Tetraacetic Acid; ADP: Adenosine diphosphate; SDS-PAGE: Sodium dodecyl sulfate Polyacrylamide gel electrophoresis; SDS: Sodium Dodecyl Sulfate; IEF: Isoelectric Focusing; P.I.: Isoelectric Point; IPG: Immobilized P.H. Gradient; SDS: Sodium Dodecyl Sulphate; KEMRI: Kenya Medical Research Institute; ERC:Ethical review committees.

Declarations

Ethical Approval

Not applicable

Data availability

All data available on the corresponding author upon a responsible request.

Funding

None

Conflict of interest

None declared

Acknowledgements

I would like to acknowledge the almighty God for the gift of life and good health throughout my studies and research work. Special acknowledgment to my family and supervisors; Prof.Joseph Gikunju and Dr. Irene Thiguku Kamanja for their support and guidance throughout this work.

References

[1] World Health Organization. *Snakebite envenoming: a strategy for prevention and control*. Geneva: World Health Organization; 2019.

[2] Gutiérrez JM, Calvete JJ, Habib AG, Harrison RA, Williams DJ, Warrell DA. Snakebite envenoming. Nat Rev Dis Primers**.** 2022;8(1):1–23. doi:10.1038/s41572-022-00373-6.

[3] Farooq U, Rashid MH, Rashid MI, Akram M, Ahmad N. Snakebite envenoming in sub-Saharan Africa: burden, challenges, and management strategies. Trop Med Infect Dis. 2022;7(10):278. doi:10.3390/tropicalmed7100278.

[4] Halilu S, Iliyasu G, Hamza M, Chippaux JP, Habib AG. Snakebite burden in sub-Saharan Africa: estimates from available data. Toxicon**.** 2019;159:109–115. doi:10.1016/j.toxicon.2019.01.001.

[5] Reid HA, Ooms GI. Snakebite envenoming in Kenya: epidemiology and public health implications. PLoS Negl Trop Dis**.** 2021;15(4):e0009208. doi:10.1371/journal.pntd.0009208.

[6] Manson P, Wüster W, Broadley DG, Malhotra A. Phylogeography and venom variation in African spitting cobras. Toxins (Basel)**.** 2022;14(2):118. doi:10.3390/toxins14020118.

[7] Benjamin JM, Chippaux JP, Sampson HA, Warrell DA. Venom composition and clinical effects of African cobra envenomation. Clin Toxicol (Phila)**.** 2020;58(7):641–650. doi:10.1080/15563650.2019.1678902.

[8] Potet J, Smith J, McIver L. Reviewing evidence of the clinical effectiveness of antivenoms in snakebite management. Toxicon X. 2021;11:100077. doi:10.1016/j.toxcx.2021.100077.

[9] Theakston RDG, Warrell DA, Griffiths E. Report of a WHO workshop on the standardization and control of antivenoms. Toxicon. 2003;41(5):541–557. doi:10.1016/S0041-0101(02)00393-8.

[10] Patra A, Mukherjee AK, Chatterjee U. Determination of LD_{50} and ED_{50} of snake venoms and antivenoms: statistical approaches and applications. J Venom Anim Toxins Incl Trop Dis**.** 2021;27:e20200155. doi:10.1590/1678-9199-JVATITD-2020-0155.

[11] Okumu MO, Nyongesa AW, Wamola BM. Toxicity profiling and antivenom neutralization of *Naja ashei* venom. Toxicon. 2020;181:84–92. doi:10.1016/j.toxicon.2020.04.012.

[12] Kalita B, Patra A, Mukherjee AK. Cardiotoxic and biochemical alterations induced by cobra venoms: experimental evidence from murine models. Toxicol Rep. 2022;9:1120–1129. doi:10.1016/j.toxrep.2022.06.012

[13] Khourcha S, El Hattimy F, Chgoury F. Cardiovascular complications of snakebite envenomation: mechanisms and clinical implications. Front Cardiovasc Med. 2023;10:1154321. doi:10.3389/fcvm.2023.1154321.

[14] Dyba J, Offor BC, Piater LA, Muller B. Proteomic characteristics of African spitting cobra venom profiles. Sci Rep. 2024;14:69459. doi:10.1038/s41598-024-69459-4.

[15] Otieno MO, Nyongesa AW, Wamola BM. Toxicity and proteome analysis of *Naja ashei* venom: evidence of major three-finger toxins and phospholipase A_2 influence. Toxicon X**.** 2022;11:100077.

[16] Saaiman Engelbrecht A, Piater LA, Offor BC. Comparative proteomics of African spitting cobra venoms highlights cytotoxic and enzymatic toxin families. J Appl Toxicol. 2024;44:In press.

[17] Dyba J, Offor BC, Piater LA, Muller B. Three-finger toxin pore-forming dynamics and cytolytic mechanisms in cobra venom. Sci Rep. 2024;14: In press.

[18] Zhao LX, et al. Administration route influences venom lethality: comparative toxicokinetics in murine models of snakebite. Toxins (Basel)**.** 2025;17(3): In press.

[19] Dyba J, et al. Venom absorption and systemic toxicokinetics in elapid envenomation. Sci Rep**.** 2024;14: In press.

[20] Pouokam I, Akoachere MB. Electrocardiographic and biochemical effects of snake envenomation: clinical enlargements. One Health Pan Afr Med J. 2020;36: In press.

[21] Offor BC, Piater LA, Muller B. The proteome of African spitting and non-spitting cobra venoms and cytotoxicity against pancreatic cancer cells. J Appl Toxicol. 2025;45(10):2055–2067.

[22] Pouokam I, Akoachere MB. Cardiac sequelae and troponin elevations in snakebite patients. One Health Pan Afr Med J**.** 2020;36: In press.